Two-band electron transport in a double quantum well

R. Fletcher,[1] M. Tsaousidou,[2] T. Smith,[1] P. T. Coleridge,[3] Z. R. Wasilewski,[3] and Y. Feng[3]
[1]*Physics Department, Queen's University, Kingston, Ontario, Canada, K7L 3N6*
[2]*Materials Science Department, University of Patras, Patras 26 504, Greece*
[3]*Microstructural Sciences, National Research Council, Ottawa, Canada K1A OR6*
(Received 26 November 2004; published 12 April 2005)

The carrier densities and mobilities have been measured for the first two populated subbands in a GaAs double quantum well (DQW) as a function of the top gate voltage V_g. The densities and quantum mobilities (μ_i^q, $i=1,2$) were obtained from the de Haas-Shubnikov oscillations. The transport mobilities (μ_i^t) were determined from the semiclassical low-field magnetoresistance with intersubband scattering taken into account. At 0.32 K the experimental data on both μ_i^t and μ_i^q, as a function of V_g, lie on two curves which cross at the resonance point as expected from theoretical considerations. At 1.09 K and 4.2 K the μ_i^t curves no longer cross at resonance, but show a gap. The reason for this is not known. The mobilities have been calculated in the low-temperature limit within the Boltzmann framework by assuming that they are limited by scattering due to ionized impurities located at the outside interfaces. The assumption of short-range scattering is justified by the relatively small value of the ratio μ_i^t/μ_i^q that is measured in the present system. The theoretical values obtained for μ_i^t and μ_i^q are in reasonable agreement with the experiment for all values of V_g examined. We have also calculated the resistivity and intersubband scattering rates of the DQW as a function of V_g and again find good agreement with measured values.

DOI: 10.1103/PhysRevB.71.155310 PACS number(s): 73.40.Kp

I. INTRODUCTION

The resistivity of double quantum wells (DQWs) coupled by tunneling was investigated by Palevski *et al.*[1] in 1990 and since that time there have been numerous further studies. When the two wells in a DQW are adjusted to be symmetric so that the energy levels in their bands coincide, the wave functions in the wells are strongly mixed to form symmetric and antisymmetric states separated by an energy gap that depends on the barrier between the wells, and the electrons have equal probabilities of being in either well. As the system moves away from symmetry, the two bands become progressively localized in one or the other of the wells.

When such wells are connected in parallel they show a "resistance resonance" around the symmetry point. This is most pronounced when the electron-impurity (e-i) scattering probabilities of the carriers in the two wells are very different, as in the present experiments. Well away from resonance, the carriers in each well contribute to the current essentially independently, and those in the high-mobility well dominate the current, thus keeping the parallel resistance low. At resonance the carriers spend equal time in each well (providing the tunneling time is short compared to the scattering time) so that the impurity-scattering rate for all carriers is dominated by the rate in the low-mobility well. Thus the resistivity rises at this point.

Such resonances have been extensively studied in a variety of DQWs.[1–5] In some experiments the carrier densities in the two bands have been determined using the de Haas-Shubnikov (deHS) oscillations in a perpendicular magnetic field (e.g., Refs. 4–6), and this is the method we have followed. The new feature of the present experiments is that we have also measured the transport and quantum mobilities of the carriers in each of the two bands of the DQW. The former were obtained from the semiclassical magnetoresistance in very low perpendicular fields, and the latter were obtained from a detailed analysis of the deHS oscillations.

The densities in each band have been calculated using a simple model based on the solution of Schrodinger's equation for two coupled, square quantum wells. Despite the simplicity of the model the agreement with measured values is very good. We have also calculated the transport mobilities of the two-band system at low temperatures within a Boltzmann framework. The calculations were made for a model in which the impurities are located at the outer interfaces of the DQW, because it was found that the distribution expected from the growth sequence could not describe the measured mobilities. From the calculated values of the densities and the transport mobilities of each band we have estimated the zero-field resistivity of the DQW. Finally, the quantum mobilities for each band were calculated from Fermi's golden rule. All of the experimental results were reproduced reasonably well with the model.

II. SAMPLE

The present experiments made use of a sample with two 18-nm-wide GaAs wells separated by a 3.4 nm barrier of $Al_{0.67}Ga_{0.33}As$. The electrons were provided by a δ-doped Si layer on each side of the wells and separated from them by 120 nm of $Al_{0.67}Ga_{0.33}As$. The relative energies of the wells were adjusted by a top gate which comprised a gold film insulated by 30 nm of SiO_2. To a good approximation, when both wells were occupied the gate raised or lowered the energy of only the well closest to the sample surface (the upper well) with the carrier density in the bottom well being almost constant. The gate allowed the density in the upper well to be varied from zero to at least 2 times the density in the lower well.

 ©2005 The American Physical Society

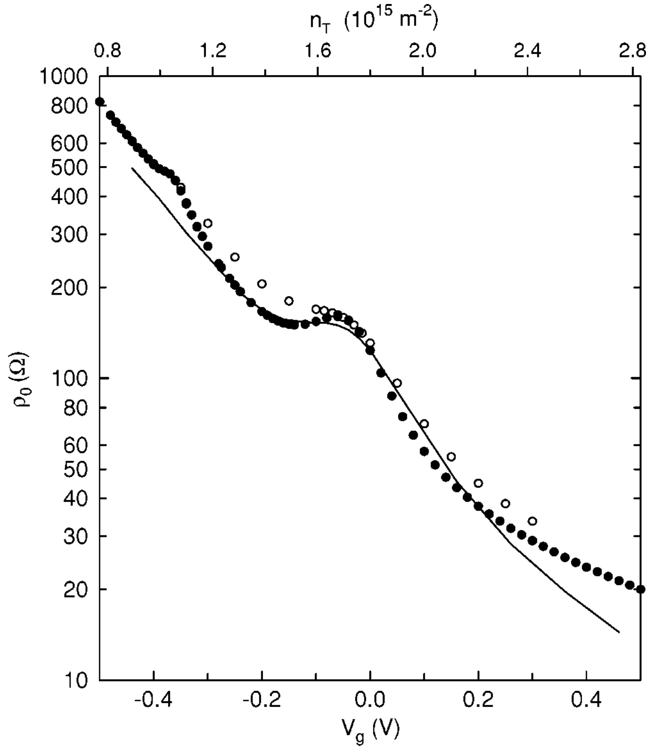

FIG. 1. The zero-field resistivity, ρ_0, as a function of gate voltage V_g and total carrier concentration n_T. The resonance is near V_g=−0.04 V. The filled and open circles are data at 0.32 K and 4.2 K, respectively. The line was calculated using the model described in the text.

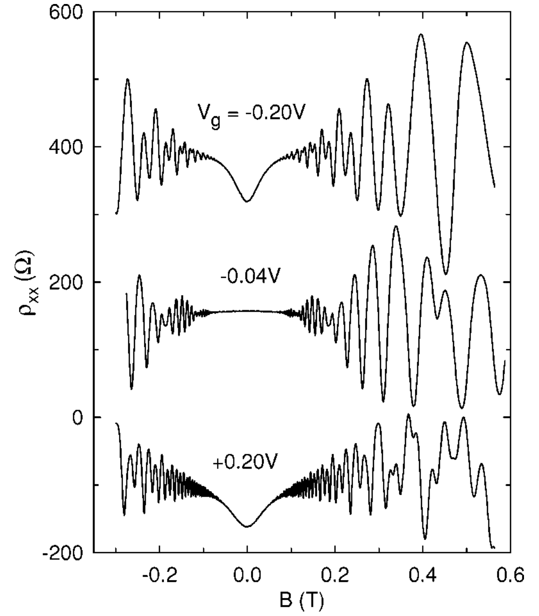

FIG. 2. Examples of data on the resistivity ρ_{xx}, at 0.32 K as a function of magnetic field B at various fixed gate voltages V_g. The top curve is offset by +150 Ω and the bottom by −200 Ω.

III. EXPERIMENTAL TECHNIQUES AND RESULTS

The longitudinal resistivity was measured by standard dc four-terminal methods with a resolution of a few nV s. Measurements were made as a function of gate voltage V_g and magnetic field B at fixed temperatures of T=0.32 K, 1.09 K, and 4.2 K. The current was typically about 50 nA, chosen to give no observable electron heating as determined from the deHS oscillations. The resistivity ρ_0 as a function of V_g and the total carrier density n_T at 0.32 K and 4.2 K are shown in Fig. 1. Both curves exhibit a resonance at $V_g = -0.04 \pm 0.01$ V ($n_T = 1.65 \pm 0.05 \times 10^{15}$ m^{-2}) and, in agreement with previous work, the resonance broadens as the temperature is increased. The broadening is barely visible at 1.09 K, and so these data are not shown.

As V_g is decreased, the background resistivity rises smoothly. This is primarily caused by the decreasing density of carriers in the upper well that have a higher mobility than those in the lower well away from the resonance. Near $V_g = -0.35$ V there is a small kink in the curve that corresponds to the point at which the upper well is emptying. Charlebois *et al.*[5] show more data on the resistance resonance over a wider range temperatures for another sample taken from the same wafer. (Note that their gate had a thicker SiO_2 layer.)

The resistivity ρ_{xx} was also measured as a function of the perpendicular magnetic field B at many different fixed values of V_g. Some examples of data at 0.32 K are shown in Fig. 2. For analysis purposes we consider each of these curves to be the sum of a semiclassical background ρ_{xx}^{sc} plus a quantum-oscillatory part ρ_{xx}^{osc}. At V_g=0.2 V and −0.2 V, a clear minimum in the resistivity at B=0 is seen for each curve; this is due to ρ_{xx}^{sc} and arises from two groups of carriers with different mobilities. However, at V_g=−0.04 V (i.e., at resonance) where the wells have the same mobility, there is no observable minimum. This is in accordance with expectations for the behavior of the semiclassical magnetoresistance when both groups of carriers have the same mobility, as will become clearer in Sec. III B. Under these conditions a weak maximum is visible, which we will also return to later. The deHS oscillations, i.e., in the component ρ_{xx}^{osc}, become visible in these data at ~0.07 T, a field at which ρ_{xx}^{sc} is beginning to saturate. At 1.09 K the oscillations are strongly damped, and by 4.2 K they are negligible over the field range of interest.

A. Analysis of deHS oscillations

As expected, over practically the whole range of gate voltage, the deHS oscillations indicate two oscillation frequencies, f_i, ignoring sum and difference frequencies and harmonics. After removing most of the background, the resulting oscillations were Fourier transformed and the densities n_i of the electrons in the two bands were obtained from the usual expression $n_i = 2ef_i/h$.

Although the random scatter on n_i obtained by Fourier analysis was reasonably low, it was found that it could be further reduced by directly fitting the oscillations to the standard expression,[7,8]

$$\rho_{xx}^{osc} = \sum_{i=1,2} A_i D(X) \exp\left(-\frac{\pi}{\mu_i^q B}\right) \cos\left(\frac{2\pi f_i}{B} + \phi_i\right), \qquad (1)$$

where A_i and ϕ_i are constants and $D(X) = X/\sinh X$ is the thermal damping factor with $X = 2\pi^2 k_B T/\hbar\omega_c$, k_B being the

Boltzmann constant, ω_c being the cyclotron frequency, and μ_i^q are the quantum mobilities. Clearly this analysis has the additional advantage of allowing the quantum mobilities for the two bands to be obtained. The term $\exp(-\pi/\mu_i^q B)$ accounts for the broadening of the Landau levels due to impurity scattering, and it is usually referred to as the Dingle factor. The Dingle temperature T_D is another standard measure of Landau-level broadening and the Dingle factor is often written as $\exp(-2\pi^2 k_B T_D/\hbar\omega_c)$.

The analysis procedure involved first removing any residual background by filtering, using Fourier transform methods; at the same time any sum and difference frequencies[8] and harmonics were also removed. The fitting was done using nonlinear least-mean-squares iterative techniques with the parameters A_i, f_i, μ_i^q, and ϕ_i as unknowns. To increase the sensitivity of the fitting to the low-field data, the weighting of the data points was increased by a factor of 10 at fields <0.22 T. The fits were always excellent over the full-field range. Occasionally there were observable deviations between the fitted curves and the data at the highest fields, but this was expected, because Eq. (1) becomes inaccurate when the oscillation amplitude is large; this was one of the reasons for strongly weighting the low field oscillations. The same analysis was carried out for data at both 0.32 K and 1.09 K. Interestingly, at 1.09 K the Fourier transforms did not have enough resolution to clearly separate the two frequencies through the resonance region, but the direct fits did allow this. By 4.2 K there were insufficient oscillations for an analysis to be made.

The values of n_i and $n_T = n_1 + n_2$ as functions of V_g obtained from this procedure are shown in Fig. 3. The various curves for n_i appear to be very similar at the two temperatures, but the higher temperature data give consistently slightly higher values. At 0.32 K we find $n_T = (1.71\pm0.01) + (2.08\pm0.02)V_g$ 10^{15} m^{-2} with V_g in volts, and at 1.09 K, $n_T = (1.74\pm0.01) + (2.08\pm0.04)V_g$ 10^{15} m^{-2}. The same figure also shows some values of n_T obtained from the Hall data that obey $n_T = (1.78\pm0.01) + (2.10\pm0.01)V_g$ 10^{15} m^{-2} at 1.09 K.

The differences in n_T between the various data sets may or may not be real. They could be due to minor irreproducibilities in the impurity ionization on different cooldowns. It is also possible that the quoted errors for the deHS evaluations do not adequately reflect the true uncertainties. The fits at 0.32 K were made down to about 0.07 T. It is difficult to control errors in B to better than 0.002 T, so the upper limit on $1/B$ could be inaccurate by $\sim$2–3 %. On the other hand, the Hall data are essentially linear in B, and small errors in the field are much less of a problem.

The results on μ_i^q for the 0.32 K data are shown in Fig. 4 and, as expected, they are seen to have the form of two smooth curves crossing at the resonance point. The corresponding values of T_D are in the range of 0.1–0.5 K for these data. The 1.09 K fits (not shown) also yield values of T_D, but the uncertainties are much larger, typically 0.1–0.2 K, because of the reduced lengths of the data sets. Within these uncertainties the results generally agree with those obtained from the 0.32 K data.

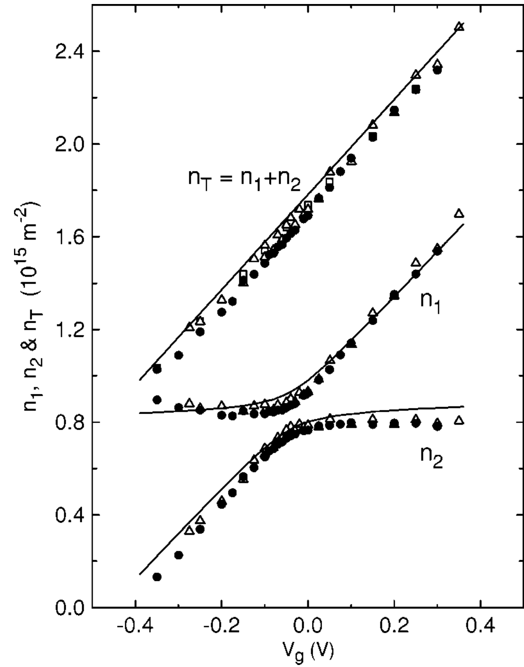

FIG. 3. The carrier densities as functions of gate voltage V_g. The filled circles and open triangles are results evaluated from the deHS data at 0.32 K and 1.09 K, respectively. The open squares are from the Hall data at 1.10 K. The lines were calculated using the model described in the text.

B. Analysis of semiclassical background

The two-band model for the semiclassical magnetoresistivity in a perpendicular magnetic field is well known (e.g., see Ref. 9). It assumes that two groups of carriers exist with densities n_i and transport mobilities μ_i^t $(i=1,2)$, and that the two groups carry current independently. If we associate the two groups with the two bands in the DQW, then the last

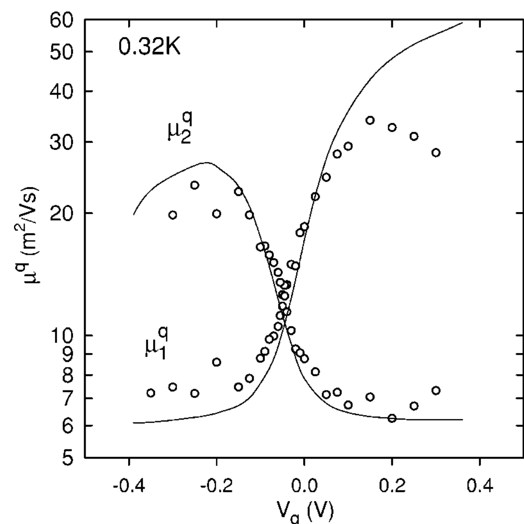

FIG. 4. The quantum mobilities μ^q as a function of gate voltage, V_g. The open circles were obtained from the deHS data at 0.32 K. The lines were calculated by using Eqs. (9)–(16) as explained in the text.

assumption is not satisfied around the resonance point, where a significant fraction of the scattering is intersubband. It has been shown[10] that the two-band model can be modified to take interband scattering into account. The resulting semiclassical resistivity ρ_{xx}^{sc} can be written

$$\rho_{xx}^{sc} = \rho_0 \left[1 + \frac{r n_1 n_2 \mu_1^t \mu_2^t (\mu_1^t - \mu_2^t)^2 B^2}{(n_1 \mu_1^t + n_2 \mu_2^t)^2 + (r n_T \mu_1^t \mu_2^t)^2 B^2} \right], \qquad (2)$$

where ρ_0 is the zero-field resistivity$=1/(n_1\mu_1^t + n_2\mu_2^t)e$. The dimensionless parameter r takes into account interband scattering, and when $r=1$ this equation reduces to the usual two-band result for two independent bands. In a DQW we expect r to approach unity well away from the resonance condition, because then the wells behave almost independently. The model predicts a positive magnetoresistivity which saturates when the magnetic field satisfies the semiclassical, high-field condition for both groups of carriers, $\mu_i^t B \gg 1$. Clearly, if the two groups have exactly the same mobility, then there is no magnetoresistance from this mechanism.

We have analyzed ρ_{xx}^{sc} at low magnetic fields using Eq. (2). The usual technique reported in the literature for analyzing such data has been to fit the relative resistivity $(\rho_{xx}^{sc} - \rho_0)/\rho_0$. However, we have fitted the full expression because the absolute value of ρ_0 provides a much stronger constraint on the allowed values of the mobilities than do the relative resistivity values. In this regard, when measuring the dc voltage across the sample to obtain the resistivity during a field sweep, there was always a small offset which was determined and eliminated from the signal. As a check, the resistivity at the zero field was also measured, using current reversals to automatically eliminate the offset, and, if necessary, these results were used to normalize the data obtained during the field sweeps.

The values of n_i for the two bands were taken directly from the results of fitting the deHS oscillations at 0.32 K. There are other points about the analysis that should also be mentioned. Clearly in Fig. 2 the oscillations and semiclassical behavior overlap at 0.32 K (but this is not the case at 1.09 K where the oscillations are much weaker, nor at 4.2 K where they are negligible). When the deHS oscillations became relatively large, the curve fitted to the semiclassical part could be significantly affected, depending on precisely where the data set was terminated on an oscillation. To minimize this problem the 0.32 K data were smoothed to eliminate the lowest field oscillations so that fits up to about 0.15–0.20 T became possible. This was done by averaging the data around each point using Gaussian weighting,[11] the width of the Gaussian being chosen to eliminate the low-field oscillations but to have no observable effect on ρ_{xx}^{sc}.

To obtain the best fits it was also found necessary to include an extra resistivity contribution of the form,

$$\rho_{xx}^{ex} = aB + bB^2. \qquad (3)$$

The first term was very small ($\lesssim 1\%$ of ρ_0 over the field range of interest) and it arose because the data were not precisely even in B, presumably due to a small admixture of the Hall resistivity. It was noticeable only when the mobilities of the two bands were almost the same.

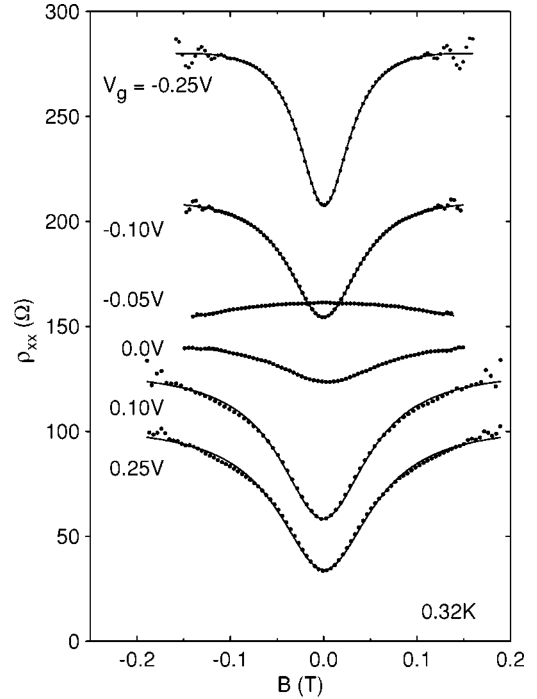

FIG. 5. Examples of the experimental, semiclassical resistivity ρ_{xx}^{sc} at various fixed gate voltages V_g as a function of the magnetic field B at 0.32 K. The filled circles are the measured values and the lines are fitted curves using Eqs. (2) and (3). The experimental data have been smoothed to reduce the deHS oscillations (as explained in the text).

The coefficient b in the quadratic term was always negative. This term was usually not resolved with any accuracy, and was not readily visible away from the resonance. The magnitude is roughly $1.0 \pm 0.5\ \Omega/T^2$ over most of the range of gate voltages, but in the region around the resonance it approximately doubles. A term of this type is often seen in magnetoresistance experiments and has been ascribed to Coulomb interactions.[12] If this were the case here, it would exhibit a log T dependence, but the scatter in our data does not allow this to be tested. Note that Eq. (2) is also approximately quadratic (and positive) near $B=0$, but the factor bB^2 gave a much smaller contribution, except close to resonance, and in practice the two components were independent of each other. Thus a full fit had five free parameters comprising μ_1^t, μ_2^t, r, a, and b. However, the resulting values of μ_i^t were hardly changed when we set $a=0=b$, though the fitted curves were visibly worse.

Some examples of the (smoothed) experimental data for ρ_{xx} and the fitted curves are shown in Fig. 5. The fitted curves were always very good representations of the data. We also tried fitting with the standard model[9] with $r=1$. This gave much poorer fits around the resonance region, as expected, because the interband scattering is strong here, but well away from resonance any difference between the two fits became very small. However, the transport mobilities determined by both types of fit show a similar behavior over the whole range of densities.

We note that Eq. (2) always allows two possible sets of solutions[13] when fitting any experimental curve (i.e., two dif-

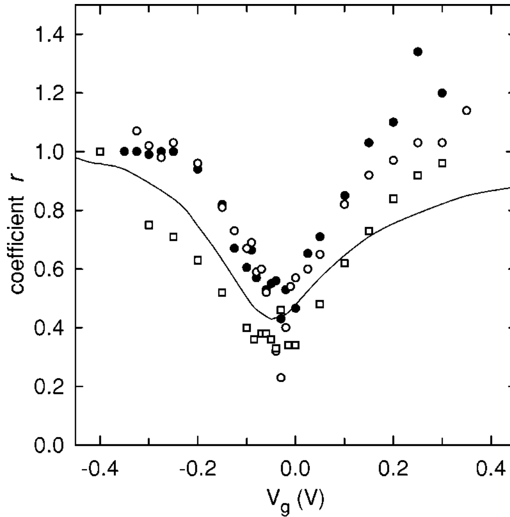

FIG. 6. The coefficient r in Eq. (2) as a function of gate voltage V_g. The symbols are experimental data: open circles are 0.32 K, filled circles are 1.09 K, and open squares are 4.2 K. The line was calculated by using Eq. (17), as explained in the text.

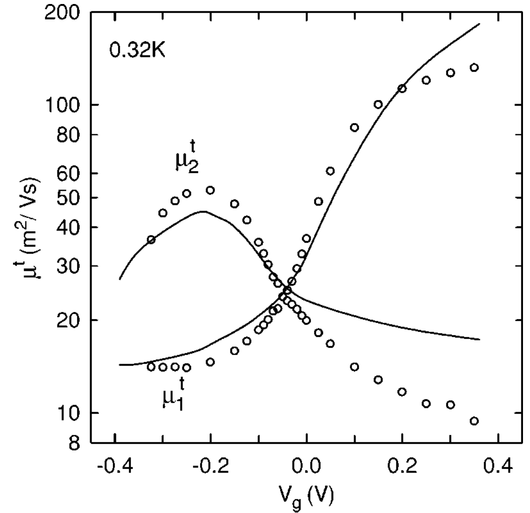

FIG. 7. The transport mobilities μ^t as a function of gate voltage V_g. The open circles are the measured quantities at 0.32 K evaluated from the semiclassical magnetoresistivities. The lines were calculated by using Eqs. (7)–(15), as described in the text.

ferent sets of coefficients for μ_i^t and r), and these two sets give identical goodness-of-fits. The two sets of solutions were readily found for all experimental curves. They gave values for r and μ_i^t, which lie on different smooth curves, as a function of V_g or n_T, except at resonance where they merge, because at this point $\mu_1^t = \mu_2^t$. However, one set of solutions had an unphysical behavior for r when the system was well away from resonance, and it was discarded on this basis. The correct set gave the expected limit of $r \approx 1$ under these conditions, whereas the incorrect set had either a very large value of r ($\sim$10) or a very small value ($\sim$0.1–0.2) at $V_g \approx \pm 0.35$ V, respectively. The data for the coefficient r at the various fixed temperatures are shown in Fig. 6 as a function of V_g, and they are seen to have a minimum near resonance ($V_g = -0.04$ V).

The values for μ_i^t as a function of V_g at 0.32 K are shown in Fig. 7. They lie on two smooth curves which appear to cross at the resonance point just as the quantum mobilities do in Fig. 4. The width of the resonance as seen in Fig. 7 correlates well with that in Fig. 1. At the crossing point ($V_g = -0.04 \pm 0.01$ V) there is no sign of a dip in the measured resistivity shown in Fig. 5, indicating that the two mobilities are indeed identical here. The upper well has the higher mobility across the whole range. However, at large negative gate voltages ($\lesssim -0.35$ V) the upper well empties and the magnetoresistivity again shows no minimum.

The transport mobilities in Fig. 7 are always higher than the quantum mobilities in Fig. 4, which is typical of modulation-doped GaAs heterostructures.[7] Often in GaAs systems the ratio μ^t/μ^q is a factor of 10 or more, but here it is typically 2–3, implying that the carriers are subject to more large-angle scattering than was expected from the modulation doping used. Furthermore, the upper well has a consistently higher mobility than the lower well, which is inconsistent with the symmetric doping used in the growth. However, although the wells were designed to be symmetrically modulation doped, in practice[14] there is often a movement of the dopant atoms with the growth front which results in a tail of Si atoms from the lower doping layer extending to both quantum wells, but with the higher density in the lower well. This would explain both the higher mobility of the top well and the low ratio of μ^t/μ^q.

The same analysis was also carried out for the data at 1.09 K and 4.2 K, and the results are shown in Figs. 8(a) and 8(b). In both cases we used values of n_i determined from the analysis of ρ_{xx}^{osc} at 0.32 K. For comparison purposes we also analyzed the 1.09 K data using n_i determined from ρ_{xx}^{osc} at the

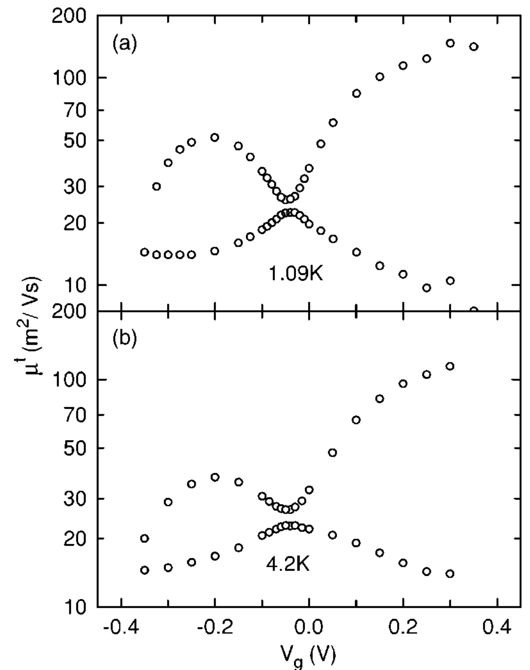

FIG. 8. The experimental transport mobilities μ^t evaluated from the semiclassical magnetoresistivities as a function of gate voltage V_g at 1.09 K (upper panel) and 4.2 K (lower panel).

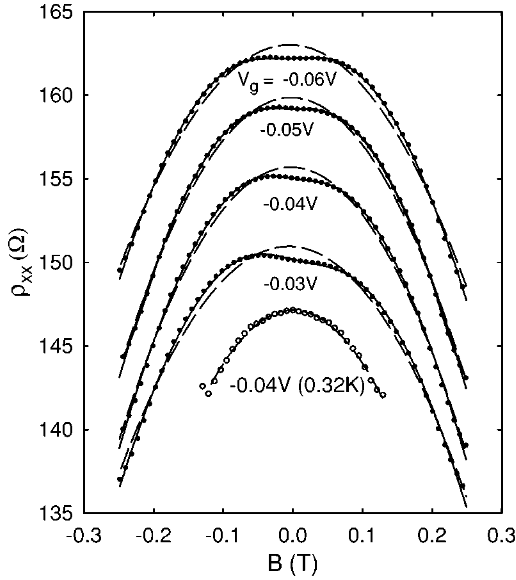

FIG. 9. The solid circles in the four topmost curves are the experimental ρ_{xx} data at 4.2 K at various fixed gate voltages V_g around the resonance point (V_g=−0.04 V) as a function of the magnetic field. The lowest curve shows the experimental data at 0.32 K (open circles) at the resonance point. The solid lines are fits to the 4.2 K data using Eqs. (2) and (3). The dashed lines are fits at both temperatures, which assume that $\mu_1^t=\mu_2^t$ so that Eq. (2) yields only ρ_0. This latter form gives an adequate fit to the 0.32 K data, showing that at resonance $\mu_1^t=\mu_2^t$. In contrast, all the 4.2 K curves show a minimum at the origin, which implies that there is no point at which $\mu_1^t=\mu_2^t$. The asymmetry in the data is due to the term aB in Eq. (3).

same temperature; this made no obvious difference to the resulting transport mobilities, except that the random scatter was much higher.

At these higher temperatures the resulting curves no longer cross at the resonance point. This is an unexpected development, but it is confirmed by the simple observation that Eq. (2) shows that a point of no positive magnetoresistance only requires $\mu_1^t=\mu_2^t$, the precise values of n_1 and n_2 not being important. We can find such a point in the data at 0.32 K, but not at 1.09 K and 4.2 K. The low-field behavior of the resistivity for various gate voltages around the resonance condition is shown in Fig. 9 for the 4.2 K data, where all the curves show positive magnetoresistance around the origin, and for comparison also for 0.32 K at resonance, where the curve shows no positive magnetoresistance. We recall that n_1 and n_2 show no unusual behavior as one increases the temperature from 0.32 K to 1.09 K (see Fig. 3) suggesting that whatever causes the mobility gap at resonance, it does not influence n_i in a significant way.

Another interesting feature of the 4.2 K data in Fig. 8(b) is that the width of the resonance is clearly wider than that indicated by the 0.32 K data in Fig. 7. This temperature-induced broadening correlates well with that of the resistance resonance in Fig. 1. At 1.09 K [Fig. 8(a)] there is no noticeable increase in the resonance width, and this is also the case for the 1.09 K resonance data (not shown in Fig. 1).

IV. THEORETICAL RESULTS AND COMPARISON WITH THE EXPERIMENTAL DATA

A. Electron densities of the first two subbands

The electron wave functions and the corresponding energy eigenvalues that describe the lowest two states in a DQW are

$$\Phi_{i\mathbf{k}}(x,y,z)=\phi_i(z)\exp(\mathbf{k}\cdot\mathbf{r})/\sqrt{A}, \quad (4)$$

and

$$E_{i\mathbf{k}}=E_i+\hbar^2k^2/2m^*, \quad (5)$$

where $i=1,2$ is the subband index, $\mathbf{k}=(k_x,k_y)$ is the electron wave vector, $\mathbf{r}=(x,y)$ is the electron position in the xy-plane, and A is the sample area. The subband energies E_i and the electron wave functions $\phi_i(z)$ for the confining potential in the z direction were calculated by solving Schrodinger's equation for two square quantum wells (QWs) of width 18 nm separated by a potential barrier of width 3.4 nm. When the applied gate voltage is zero the two wells of the DQW are symmetric and their height is taken to be V_1 =310 meV. The potential barrier of the top well varies linearly with the applied gate voltage, according to the relationship $\Delta V_1=\alpha V_g$. The proportionality constant α was determined by matching the change of the density of the top well to the change of the barrier potential, where tunneling between the wells is ignored.

The wave functions for the symmetric wells are strongly mixed to form symmetric and antisymmetric states separated by an energy gap that depends on the barrier between the wells, and the electrons have equal probabilities of being in either well; this is the resonance condition. By varying the gate voltage in the top well the system moves away from resonance and the two bands become progressively localized in one or the other of the wells. Examples of calculated wave functions at various values V_g for the present sample are shown in Fig. 10, where the solid lines correspond to the symmetric state and the dashed lines to the antisymmetric state. Note that in the calculations the resonance condition occurs at V_g=0 V, while in the experiments it occurred at V_g=−0.04 V.

For degenerate systems the electron density in the ith subband is given by $n_i=(m^*/\pi\hbar^2)(E_F-E_i)$ where E_F is the Fermi level. E_F can be readily estimated from the relationship,

$$E_F=\frac{n_T\pi\hbar^2}{2m^*}+\frac{E_1+E_2}{2}, \quad (6)$$

where $n_T=n_1+n_2$ is the total density. In order to estimate the individual band densities n_1 and n_2 we put in Eq. (6) the total electron density obtained from the Hall measurements.

The calculated values of the electron densities n_i for each subband are shown in Fig. 3. For comparison with the experimental results, the theoretical curves have been shifted by −0.04 V along the horizontal axis, so that the resonance position coincides with that experimentally observed.

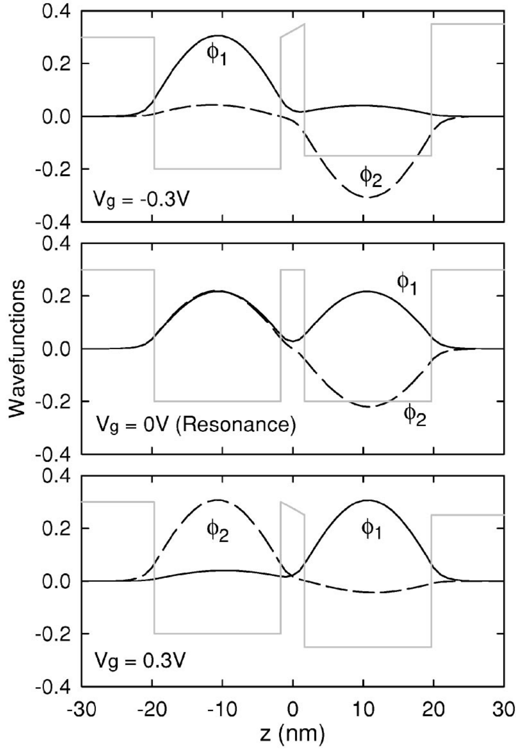

FIG. 10. Examples of calculated wave functions in the DQW at three fixed gate voltages V_g. The solid lines correspond to the symmetric state and the dashed lines to the antisymmetric state. The locations of the two wells (and their relative depths, not to scale) are indicated by gray lines.

B. Transport and quantum mobilities of the individual subbands

The transport mobility of the ith subband is $\mu_i^t = e\tau_i^t/m^*$, where τ_i^t is the elastic relaxation time due to electron scattering by ionized impurities. The relaxation times τ_i^t were obtained by solving the Boltzmann equation for a system with two occupied subbands. We have evaluated the results only in the low-temperature degenerate limit, where only electrons at the Fermi surface contribute to the relaxation times and conductivity. We obtained $\tau_i^t(E_F)$ by solving the following system of two linear equations:[10,15,16]

$$\begin{aligned} \tau_1^t K_{11} + \tau_2^t K_{12}\left(\frac{E_{F2}}{E_{F1}}\right)^{1/2} &= 1, \\ \tau_2^t K_{22} + \tau_1^t K_{12}\left(\frac{E_{F1}}{E_{F2}}\right)^{1/2} &= 1, \end{aligned} \tag{7}$$

where $E_{Fi}=E_F-E_i$ and K_{ij} are the components of the scattering matrix K given by

$$K_{ij} = \sum_{k=1}^{2} \Gamma_{ik}^0 \delta_{ij} - \Gamma_{ij}^1. \tag{8}$$

The transition rates Γ_{ij}^0 and Γ_{ij}^1 are given by the expressions,[17]

$$\Gamma_{ij}^0 = \frac{m^*}{\pi\hbar^3}\int dz_n N_{imp}(z_n)\int_0^\pi d\theta |V_{ij}(q,z_n)|^2, \tag{9}$$

and

$$\Gamma_{ij}^1 = \frac{m^*}{\pi\hbar^3}\int dz_n N_{imp}(z_n)\int_0^\pi d\theta \cos\theta |V_{ij}(q,z_n)|^2, \tag{10}$$

with θ being the scattering angle between the initial and the final states $\mathbf{k}$ and $\mathbf{k}+\mathbf{q}$ of the transition, $N_{imp}(z_n)$ being the distribution of the ionized impurities, and $V_{ij}(q,z_n)$ being the Fourier transform of the Coulomb interaction. From the conservation of energy and momentum we have[17]

$$q = \left(\frac{2m^*}{\hbar^2}\right)^{1/2}(E_{Fi}+E_{Fj}-2\sqrt{E_{Fi}E_{Fj}}\cos\theta)^{1/2}. \tag{11}$$

The Fourier transform of the Coulomb interaction is given by

$$V_{ij}(q,z_n) = \sum_{kl} V_{kl}^{bare}(q,z_n)\epsilon_{klij}^{-1}(q), \tag{12}$$

where

$$V_{kl}^{bare}(q,z_n) = \frac{e^2}{2\kappa_0\kappa q}\int_{-\infty}^{\infty}\phi_k(z)\phi_l(z)e^{-q|z-z_n|}dz. \tag{13}$$

κ_0 is the permittivity of free space, and κ is the permittivity of GaAs. In Eq. (12) $\epsilon_{klij}^{-1}(q)$ are the components of the inverse dielectric matrix in the random-phase approximation. The matrix elements $\epsilon_{klij}^{-1}(q)$ are given by

$$\epsilon_{klij}(q) = \delta_{ki}\delta_{lj} + \frac{e^2}{2\kappa_0\kappa q}F_{klij}(q)\Pi_{ij}, \tag{14}$$

where $F_{klij}(q)$ are the screening form factors,

$$F_{klij}(q) = \int dz \int dz' \phi_k(z)\phi_l(z)e^{-q|z-z'|}\phi_i(z')\phi_j(z'), \tag{15}$$

and Π_{ij} is the polarization function. In the long-wavelength limit $\Pi_{ij}\approx m^*/\pi\hbar^2$.

The quantum mobilities of the two subbands $\mu_i^q = e\tau_i^q/m^*$ are determined by the quantum lifetimes τ_i^q, which, for two occupied subbands, are obtained from Fermi's golden rule,

$$\frac{1}{\tau_i^q} = \sum_{j=1}^{2}\Gamma_{ij}^0. \tag{16}$$

In principle there are no unknowns in the calculation of τ_i^t and τ_i^q, given the ionized impurity distribution appropriate to the growth sequence of the sample. However, the experimental data on the mobilities cannot be reproduced, assuming that the only scattering comes from the ionized δ-doped Si layers 120 nm from the wells. We recall two experimental points noted in Sec. III B. The first is that the experimental ratio μ^t/μ^q is typically 2–3, whereas our calculations show that if all scattering originated from the δ-doped layers, then $\mu^t/\mu^q \sim 100$ because of the preponderance of small angle scattering. This clearly indicates that scattering centers closer to the two-dimensional electron gas (2DEG) must be present.

The second is that the wells exhibit quite different mobilities, which is inconsistent with an identical distribution of charge on each side of the wells. As noted earlier, these effects are probably mainly due to the diffusion of the dopant Si atoms, though the resulting impurity distribution is not known in any detail.

For these reasons we made the simple assumption that the ionized scatterers were located at the outer interfaces of the DQW, i.e., at distances $z_1=-19.7$ nm and $z_2=19.7$ nm from the center of the DQW ($z=0$). We calculated μ_i^t and μ_i^q as a function of the gate voltage by using Eqs. (7)–(16) and the standard material parameters for GaAs. The subband energies E_i and the electron wave functions $\phi_i(z)$ were calculated for each value of V_g as described in Sec. IV A. The best overall fits of both μ_i^t and μ_i^q were obtained with $N_{imp}(z_1) =0.11\times10^{15}$ m^{-2} (lower interface) and $N_{imp}(z_2)=0.015 \times10^{15}$ m^{-2} (upper interface). Clearly these values cannot account for the electronic densities in the 2DEG, but at this time we are unable to obtain a more realistic distribution. The results of the model calculations are shown as solid lines in Fig. 4 for μ_i^q and in Fig. 7 for μ_i^t. The theoretical results are shifted by –0.04 V along the horizontal axis to match the experimental location of the resonance point. The resistivity ρ_0 was evaluated from $\rho_0=1/e(n_1\mu_1^t+n_2\mu_2^t)$, and the results are shown in Fig. 1 as the solid line. The gate voltages for the calculated data are again shifted by –0.04 V. In all cases there is reasonable agreement with the experiment showing that the basic features of the model calculation are correct.

The effect of intersubband scattering is introduced both by the off-diagonal elements and the transition rates Γ_{12}^0 that appear in the diagonal terms of the K matrix. In order to examine this effect we calculate the r parameter that appears in Eq. (2). This parameter is given by the expression,[10]

$$r=\frac{\bar{\tau}_1\bar{\tau}_2}{\tau_1^t\tau_2^t}, \tag{17}$$

where $\bar{\tau}_1^{-1}$ and $\bar{\tau}_2^{-1}$ are the eigenvalues of the K matrix,[10]

$$\bar{\tau}_{1,2}^{-1}=\frac{1}{2}(K_{11}+K_{22})\pm\frac{1}{2}\sqrt{(K_{11}-K_{22})^2+4K_{12}^2}. \tag{18}$$

We see by the inspection of Eqs. (7) and (8) and Eqs. (17) and (18) that r becomes unity when the transition rates $\Gamma_{ij}(i\neq j)$ are set to zero. We expect that away from resonance the effect of intersubband scattering should be small. This is verified from the numerical calculations of r as $T\rightarrow0$ K, shown by the solid line in Fig. 6. The theoretical values of r are in reasonable agreement with the experimental results.

V. DISCUSSION

The calculations described in Sec. IV give a good account of all the measured quantities in the low-temperature limit. The only unknown in the theory was the microscopic distribution of the ionized impurities that gives rise to the scattering of the electrons, and so we used a model which gave the observed ratio of transport to quantum lifetime. Interestingly, the model also gave a good account of the intersubband scattering, a quantity which has been rather difficult to determine in a quantitative fashion.

Berk *et al.*[3] described the resistance resonance and the effects of an applied magnetic field parallel to the plane of the 2DEG by using an alternative microscopic model based on the Kubo formula. The model defines two lifetimes for each band, the single-particle, small-angle lifetime τ_i and the transport lifetime τ_i^{tr}. These appear to be identical to those that define the quantum mobility and transport mobility that we use here, i.e., $\mu_i^q=e\tau_i^q/m^*$ and $\mu_i^t=e\tau_i^t/m^*$. As $T\rightarrow0$ all lifetimes are determined by elastic scattering. Berk *et al.* obtained the transport lifetimes from measurements of the resistivity and the Hall coefficient well away from resonance. The broadening of the resonance as the temperature rises was ascribed by Berk *et al.* to a decreasing τ_i. They extracted τ_i by fitting the experimental resistivity as a function of the parallel magnetic field to theory and, from the resulting temperature dependence and absolute magnitude, identified the decrease as being due to electron-electron (e-e) scattering that obeys $1/\tau_{ee}\approx3.0(k_BT)^2/\hbar\varepsilon_F$.

The present data have been analyzed in a way which gives μ_i^t and μ_i^q independently. Using the above estimate of τ_{ee} for our sample would translate into a contribution to the quantum mobility due to e-e scattering of $\mu_{ee}^q=e\tau_{ee}/m^* =240/T^2$ m^2/V s at the resonance point. At 1.1 K this would result in an $\sim$6% decrease to μ^q (or an equivalent increase of 6% in T_D) between 0.32 K and 1.1 K, which is below our resolution. However, it is not clear that e-e scattering should affect T_D at all. Although the effect of e-e interactions on quantum oscillations in three-dimensional (3D) metals is known and has a long history,[18,19] we have not been able to find any information with respect to the effect of e-e scattering on T_D for either 3D or 2D systems. Experimentally, no significant temperature dependence of T_D has been detected in 3D metals.[18–20] It is known that inelastic electron-phonon scattering does not contribute to T_D, and it is possible that e-e scattering behaves in a similar way.

It is interesting that the calculation of the mobilities and the resistance resonance by the Boltzmann equation in the elastic-scattering limit, as outlined in Sec. IV, provides another theoretical approach to this problem. The two relaxation times emerge naturally, and tunneling is not introduced in any direct way, yet the results are in reasonably good agreement with the experiment. We also draw attention to similar calculations by Heisz,[21] which also gave good agreement with the experiment for the case of a parallel magnetic field.

An unexpected feature of the present experimental data is that the mobility curves do not cross at 1.09 K and 4.2 K. One possibility is that this results from the effects of the broadening of the Fermi function. We would expect this to have an effect when the thermal broadening k_BT is of the same order of magnitude as the tunneling gap. The latter is known[22] to be about 6.3 K, and so it seems likely that the 4.2 K data could be affected. Detailed calculations would be required to determine the temperature at which any effects would become visible and what form they might take.

VI. CONCLUSIONS

The present work shows that the Boltzmann approach provides a good explanation of the low-temperature transport

results measured in the present system. It would be of interest to extend it to other systems, and in particular to determine what happens when the tunneling time becomes long compared to the transport relaxation times. It would also be interesting to extend the Boltzmann calculations to finite temperatures to determine if they might provide an explanation for the broadening of the resistance resonance and the gap in the mobility curves. The alternative theory of Berk *et al.*[3] has successfully described the temperature variation of the resistance resonance and the quenching of the resonance in a parallel magnetic field by invoking e-e scattering. It is not clear whether it can also give a detailed account of the present data. Finally, we note that the present experimental and theoretical methods may also be applied to DQWs in a parallel magnetic field by using a small perpendicular field component. This would provide a detailed microscopic view of the destruction of the resonance by the field.

ACKNOWLEDGMENTS

This work was supported by a grant from the Natural Sciences and Engineering Research Council of Canada. We thank Jean Beerens at the University of Sherbrooke for providing access to pieces of the wafer. M.T. would also like to thank the University of Warwick for access to its computing facilities.

[1] A. Palevski, F. Beltram, F. Capasso, L. Pfeiffer, and K. W. West, Phys. Rev. Lett. **65**, 1929 (1990).
[2] J. P. Eisenstein, T. J. Gramila, L. N. Pfeiffer, and K. W. West, Phys. Rev. B **44**, 6511 (1991).
[3] Y. Berk, A. Kamenev, A. Palevski, L. N. Pfeiffer, and K. W. West, Phys. Rev. B **50**, 15 420 (1994); **51**, 2604 (1995).
[4] M. Slutzky, O. Entin-Wohlman, Y. Berk, A. Palevski, and H. Shtrikman, Phys. Rev. B **53**, 4065 (1996).
[5] S. Charlebois, J. C. Beerens, R. Côté, E. Lavallée, J. Beauvais, and Z. R. Wasilewski, Physica E (Amsterdam) **6**, 645 (2000).
[6] G. S. Boebinger, A. Passner, L. N. Pfeiffer, and K. W. West, Phys. Rev. B **43**, 12 673 (1991); N. E. Harff, J. A. Simmons, S. K. Lyo, J. F. Klem, G. S. Boebinger, L. N. Pfeiffer, and K. W. West, *ibid.* **55**, R13 405 (1997).
[7] P. T. Coleridge, R. Stoner, and R. Fletcher, Phys. Rev. B **39**, 1120 (1989).
[8] D. R. Leadley, R. Fletcher, R. J. Nicholas, F. Tao, C. T. Foxon, and J. J. Harris, Phys. Rev. B **46**, 12 439 (1992).
[9] J. M. Ziman, *Electrons and Phonons* (Oxford, Clarendon Press, 1960).
[10] E. Zaremba, Phys. Rev. B **45**, 14 143 (1992).
[11] P. R. Bevington, *Data Reduction and Error Analysis for the Physical Sciences* (McGraw-Hill, New York, 1969).
[12] C. W. Beenakker and H. van Houten, in *Solid State Physics*, edited by H. Ehrenreich and D. Turnbull (Academic Press, New York, 1991), p. 1.
[13] E. Zaremba (private communication).
[14] L. Pfeiffer, E. F. Shubert, and K. W. West, Appl. Phys. Lett. **58**, 2258 (1991).
[15] S. Mori and T. Ando, Phys. Rev. B **19**, 6433 (1979).
[16] E. D. Siggia and P. C. Kwok, Phys. Rev. B **2**, 1024 (1970).
[17] L. R. Gonzalez, J. Krupski, and T. Szwacka, Phys. Rev. B **49**, 11 111 (1994).
[18] D. Shoenberg, *Magnetic Oscillations in Metals* (Cambridge University Press, Cambridge, 1984).
[19] M. Springford, in *Electrons at the Fermi Surface*, edited by M. Springford (Cambridge University Press, Cambridge, 1980), p. 362.
[20] R. A. Phillips and A. V. Gold, Phys. Rev. **178**, 932 (1969).
[21] J. M. Heisz, Ph.D. thesis, Queen's University, 1998.
[22] R. Fletcher, T. Smith, M. Tsaousidou, P. T. Coleridge, Z. R. Wasilewski, and Y. Feng, Phys. Rev. B **70**, 155333 (2004).